iJRASET
International Journal For Research in Applied Science and Engineering Technology

INTERNATIONAL JOURNAL FOR RESEARCH

IN APPLIED SCIENCE & ENGINEERING TECHNOLOGY

Volume: 5 **Issue:** XII **Month of publication:** December 2017

DOI:

www.ijraset.com

Call: 08813907089 | E-mail ID: ijraset@gmail.com

International Journal for Research in Applied Science & Engineering Technology (IJRASET)
ISSN: 2321-9653; IC Value: 45.98; SJ Impact Factor :6.887
Volume 5 Issue XII December 2017- Available at www.ijraset.com

Spectroscopic and DFT Investigations on a New Macrocyclic Schiff Base Compound of o-Phenylenediamine

Sivaraman Lenin Sathya Saibaba[1], Subramaniam Kamalesu[2], Athanas Anish Babu[3], Kalaiyar Swarnalatha[4]
[1, 3, 4]*Department of Chemistry, Manonmaniam Sundaranar University, Tirunelveli-627012, India*
[2]*Department of Chemistry, Vivekanandha College of Arts and Science for Women (Autonomous), Tiruchengode-637205, India*

Abstract: ***A new Schiff base compound of 6,6'-(1E,1'Z)-(1,2-phenylenebis(azan-1-yl-1-ylidene))bis(methan-1-yl-1-ylidene)bis(2,4-diiodophenol) (PMDP) has been synthesized and good optical quality single crystals of PMDP were grown by slow solvent evaporation solution growth technique at room temperature. Synthesized compound was characterized by various analytical and spectral techniques. The crystal structure of PMDP has been determined by single crystal XRD analysis and it belongs to monoclinic crystal system with space group P21/n. The absorption and emission spectrum was recorded in the range of 200-800nm, to find the suitability of the single crystal for various optical applications. The thermal stability of the crystal was investigated from thermo gravimetric (TG) and differential thermal analysis (DTA). The structure of the synthesized PMDP was optimized using density functional theory (DFT). The molecular geometry, the highest occupied molecular orbital (HOMO), the lowest unoccupied molecular orbital (LUMO) energies and Mulliken atomic charges and molecular electrostatic potential (MEP) of the molecules are determined at the B3LYP method and standard 6-311++G (d, p) basis set starting from optimized geometry.***

Keywords: crystal growth; X-ray diffraction; crystal structure; DFT calculation; Schiff base

I. INTRODUCTION

Covalent organic-frameworks (COFs) are the prominent group of porous and ordered materials produced by condensation reactions of organic molecules. The Schiff-base chemistry or dynamic imine chemistry has been widely employed for the synthesis of COFs at a recent time. The main reason for this new tendency is based on their high chemical stability, porosity and crystallinity [1]. Schiff bases are the compounds carrying imine or azomethine (–C=N–) functional group. These are the condensation products of primary amines with carbonyl compounds and were first reported by Hugo Schiff [2, 3]. Schiff bases have a diversity of applications in numerous fields including biological, analytical and inorganic chemistry. They are also used as intermediates in organic synthesis, catalysts, dyes, pigments, corrosion inhibitors and polymer stabilizers [4]. Schiff bases have gained importance in pharmaceutical and medicinal fields due to a wide-range of biological activities like anti-inflammatory [5], antibacterial, photoinduced DNA cleaving agents [6], antifungal, anticancer and herbicidal [7,8] activities. *o*-phenylenediamine and its derivatives have been widely used in coordinate, medical, biological chemistry, spectroscopic and catalytic activities. Organic crystals have attracted a lot of attention because of their potential applications in electro-optic modulation. The conjugated electron systems in compounds with donor–acceptor benzene derivatives display extremely large second order optical nonlinearities. The conformation of molecules has been influenced by the properties of substituent at the aromatic rings in a great extent [9-11]. Most of such crystals are composed of aromatic molecules that are substituted with π-electron donors and acceptors which exhibit intramolecular charge transfer. Also, the Schiff base is of special interest in literature which shows thermo chromic and photochromic properties [12, 13]. In this work, we report on the investigation of the synthesis, crystal structure, characterization, stability and DFT calculation of the title compound in detail.

II. EXPERIMENTAL

A. Materials

o-phenylenediamine and 3,5-diiodosalicylaldehyde were purchased from Sigma–Aldrich and were used as received. All the reagents used were chemically pure and of analytical grade. Reagent grade organic solvents were purified and dried by standard procedures [14] and degassed before use.

©IJRASET (UGC Approved Journal): All Rights are Reserved

B. Instrumentation

He crystal structure of the compound PMDP was determined from the single crystal X-ray diffraction data obtained with an Oxford Xcalibur, Gemini diffractometer equipped with EOS CCD detector at 298 K. Monochromatic MoK α radiations (0.71073 Å) were used for the measurements. X-ray diffraction data were collected at room temperature. The unit cell parameters were determined. A solution was obtained readily using SHELXTL (XS) [15]. Hydrogen atoms were placed in idealized positions and were set riding on the respective parent atoms. All non-hydrogen atoms were refined with anisotropic thermal parameters. Absence of additional symmetry and voids were confirmed using PLATON [16]. The structure was refined (weighted least squares refinement on F^2) to convergence [15]. Elemental analysis was done using a Perkin-Elmer elemental analyzer. IR spectrum was obtained from a JASCO FT/IR-410 spectrometer in the range 4000-400 cm^{-1} using KBr pellets. The electronic spectra were registered on a Perkin Elmer Lambda-25 UV–Vis spectrometer. Emission measurements were done with JASCO FP-8500 spectrofluoro meter. ^{1}H NMR spectra was recorded on a Bruker AV III 400 MHz instrument using TMS as an internal reference. Electron ionization mass spectrum of the PMDP was recorded on a JEOL GCMATEII mass spectrometer. Thermal properties of PMDP were studied by thermo gravimetric analysis (TGA) which were carried out between 25º C and 800º C in nitrogen atmosphere at a heating rate of 10º C min^{-1} using NETZSCH STA 409 C/CD TGA instrument.

C. Synthesis and crystal growth

The Schiff base compound PMDP was prepared by the condensation of *o*-phenylenediamine with 3,5-diiodosalicylaldehyde in 1:2 molar ratio in methanol (40 ml). The reaction mixture was heated under reflux for 6h and then concentrated to half of the initial volume. Red solid was formed, on adding excess of anhydrous ether. The product was washed and dried at room temperature. The purity of the schiff base compound was checked by TLC (Scheme 1). Single crystals of PMDP have been grown from the saturated methanolic solution and recrystallized by slow solvent evaporation solution growth technique. Good optical quality red color single crystals have been harvested at the end of 5th day. The phtograph of the grown crystals is depicted in Fig. 1.

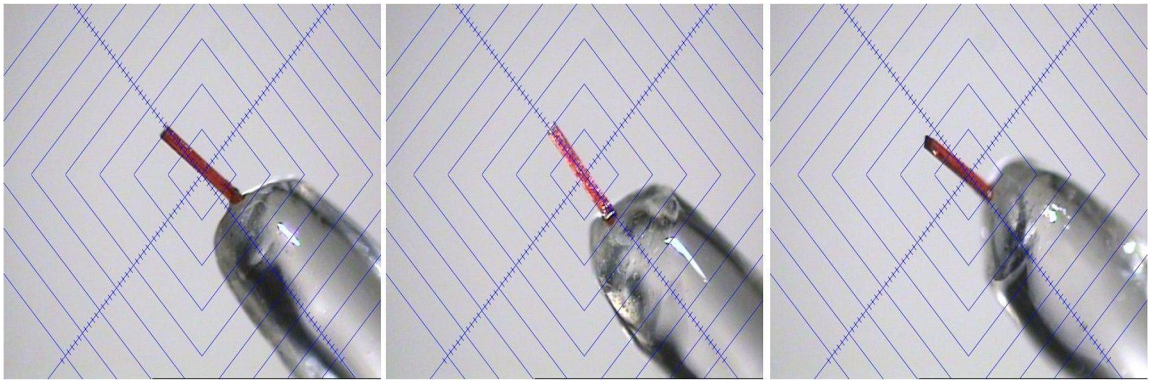

Fig. 1. shows the photograph of the grown crystals

D. Computational Methods

The entire calculations were performed using Gaussian 09 software package [17], at the B3LYP/6-311++G(d,p) level of theory. DFT methods are more beneficial owing to their accuracy and low computational cost. These properties make DFT more practical and feasible for the computations of different molecules. Transitions to the lowest excited singlet electronic states of Schiff base compound was computed by using the gradient corrected DFT with the three-parameter hybrid functional Becke3 (B3) for the exchange part and the Lee-Yang-Parr (LYP) correlation function. HOMO-LUMO energy level calculations and geometry optimization have been carried out in the present investigation, using 6-311++G(d,p) basis set with Gaussian 09W program package [18-22]. The chemical reactivity descriptors were calculated using DFT. These are very important physical parameters to understand chemical and physical activities of the synthesized molecule. Ionization potential is calculated as the energy differences between the energy of the compound derived from electron-transfer (radical cation) and the respective neutral compound; $IP_E = E_{cation} - E_n$; $IP_o = -E_{HOMO}$ and the electron affinity is computed as the energy differences between the neutral molecule and the anion molecule: $EA = E_{n-} E_{anion}$; $EA_o = -E_{LUMO}$, respectively. From these calculations the other parameters such as electronegativity (χ), electrochemical potential (μ), hardness (η), softness (σ) and electrophilicity index (ω) have been determined [23].

©IJRASET (UGC Approved Journal): All Rights are Reserved

International Journal for Research in Applied Science & Engineering Technology (IJRASET)
ISSN: 2321-9653; IC Value: 45.98; SJ Impact Factor :6.887
Volume 5 Issue XII December 2017- Available at www.ijraset.com

III RESULTS AND DISCUSSION

The purity and stoichiometric proportion of the elements (CHN) of the synthesized compound was found by elemental analysis. The micro analysis results showed that the compound PMDP contains C: 29.42% (29.30%), H: 1.38% (1.48%), N: 3.55% (3.42%). The data indicated that the experimentally determined values are in well agreement with the theoretical values (within the bracket).

A. Characterization of PMDP

1) ^{1}H-NMR Spectra: The ^{1}H NMR spectrum of PMDP was recorded in $CDCl_3$ to confirm the formation of schiff base compound (Fig. 2.). ^{1}H-NMR spectrum showed a singlet at 8.44 ppm assigned to azomethine proton (-CH=N) and a signal at 14.31 ppm characteristics of phenolic -OH proton. The multiplet signals obtained at 8.10-6.77 ppm range are due to the aromatic protons of compound.

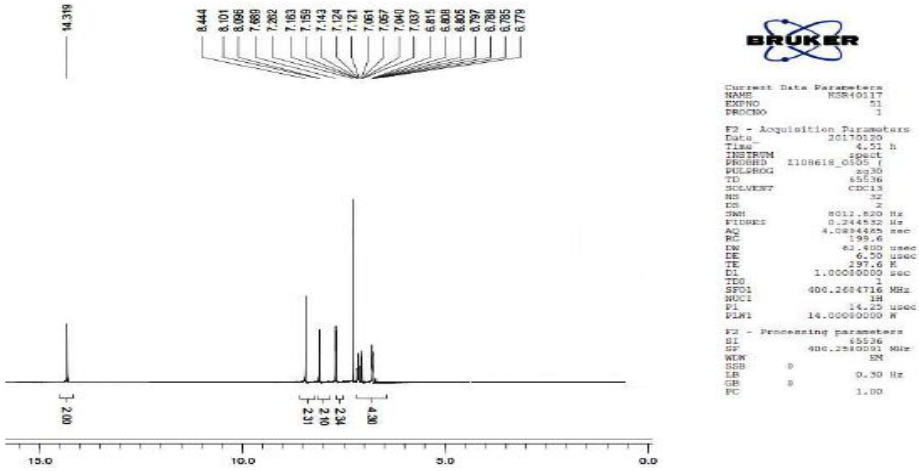

Fig. 2 NMR spectrum of PMDP

2) ESI Mass: The ESI mass spectrum of PMDP is in good agreement with the proposed molecular structure and the mass spectrum of the PMDP is shown in Fig. 3. The molecular ion peak, [M+H] appeared at m/z = 819.

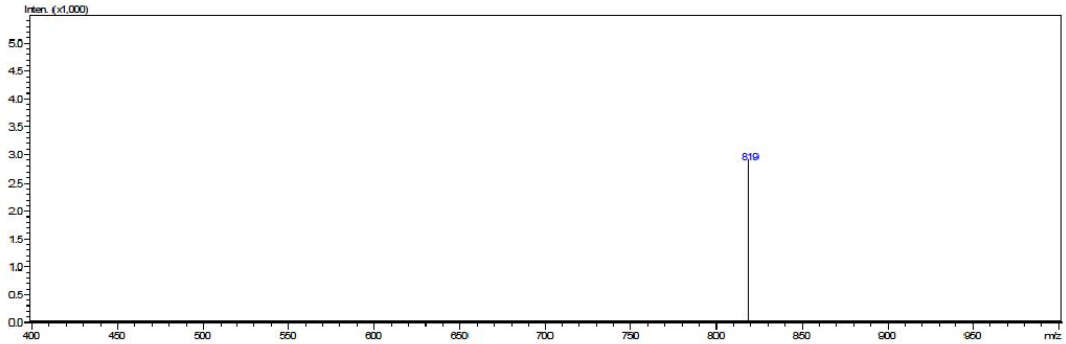

Fig. 3. ESI-Mass spectra of PMDP

3) X-ray crystallography: The ORTEP representation of PMDP is shown in Fig. 4. Relevant data collection and details of the structure refinement are summarized in Table I. The single crystal XRD data of hkl crystals indicated that the grown crystal belongs to monoclinic crystal system with P21/n space group. The cell parameters of PMDP are: a = 12.9989(16) Å, b = 8.0453(10) Å, c = 21.584(3) Å and volume is 2224.6(5) Å^3, respectively. The two azomethine bond length are N1-C7, N2-C14, and their values are 1.259(7) Å and 1.277(7) Å is in conformation with a formed C=N double bond length. The molecular conformation of the compound is given by two bond angles C(7)-N(1)-C(1), C(14)-N(2)-C(2), N(1)-C(7)-C(8) and N(2)-C(14)-C(15) C8-N2-N1-C7, C9-C8-N2-N1, N2-N1-C7-C4 and their values are 122.5(5)° 118.6(5)°,121.8(5)° and 121.9(5)° [24-25]. (CCDC 1011768).

©IJRASET (UGC Approved Journal): All Rights are Reserved

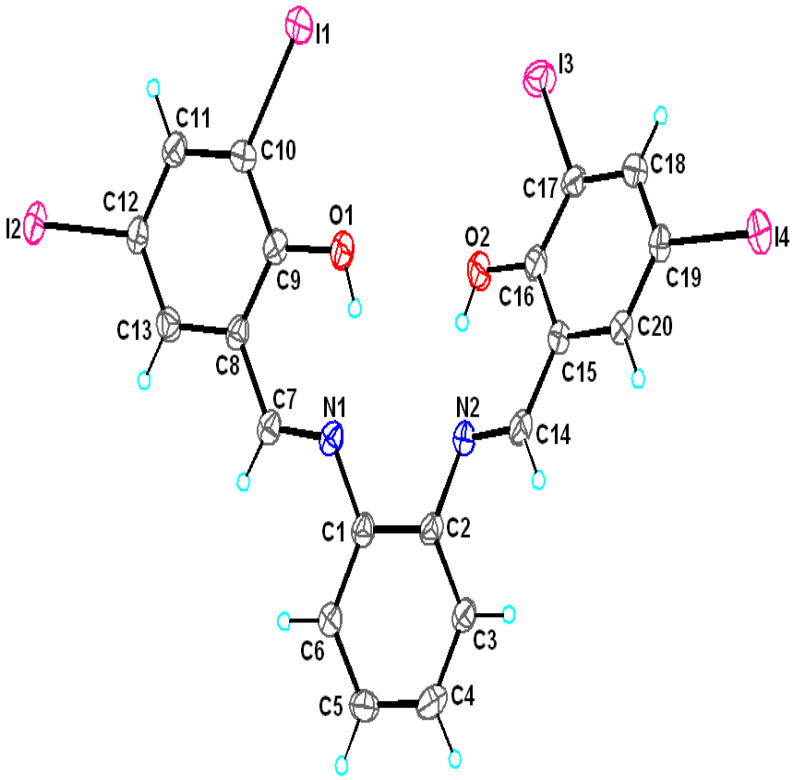

Fig. 4. ORTEP representation of PMDP

TABLE. I CRYSTAL DATA AND STRUCTURE REFINEMENT FOR kmd180.

Identification code	kmd180
Empirical formula	C20 H12 I4 N2 O2
Formula weight	819.92
Temperature	298(2) K
Wavelength	0.71073 Å
Crystal system	Monoclinic
Space group	P 21/n
Unit cell dimensions	a = 12.9989(16) Å □= 90°. b = 8.0453(10) Å □= 99.753(2)°. c = 21.584(3) Å □ = 90°.
Volume	2224.6(5) $Å^3$
Z	4
Density (calculated)	2.448 Mg/m^3
Absorption coefficient	5.621 mm^{-1}
F(000)	1496
Crystal size	0.40 x 0.24 x 0.20 mm^3
Theta range for data collection	1.71 to 28.28°.
Index ranges	-17<=h<=17, -10<=k<=10, -28<=l<=28

©IJRASET (UGC Approved Journal): All Rights are Reserved

Reflections collected	25069
Independent reflections	5366 [R(int) = 0.0434]
Completeness to theta = 25.00°	100.0 %
Absorption correction	Empirical
Max. and min. transmission	1.0000 and 0.5982
Refinement method	Full-matrix least-squares on F^2
Data / restraints / parameters	5366 / 0 / 253
Goodness-of-fit on F^2	1.153
Final R indices [I>2sigma(I)]	R1 = 0.0481, wR2 = 0.0955
R indices (all data)	R1 = 0.0630, wR2 = 0.1008
Largest diff. peak and hole	1.392 and -0.484 e.Å^{-3}

4) FT-IR spectrometry: FT-IR spectral analysis is carried out to get further structural confirmation of the synthesized compound. Fig. 5 shows the IR spectrum of PMDP and the assignment of the well defined bands is given in Table II. The bands at 3747 cm^{-1} and 3437 cm^{-1} are attributed to the O-H stretching vibration for tri substituted phenol. The azomethine nitrogen is inferred from the following observation. New strong bands appear at 1593 cm^{-1} which is attributed to the newly formed N=C bond vibration. The absorption bands at 3354 cm^{-1} is due to the aromatic C-H stretching vibrations. The C-H bending vibration of 1,2-disubstituted benzene and tetra substituted benzene moiety in the PMDP is observed at 751 cm^{-1} and 862 cm^{-1}. The peaks at 1154 cm^{-1} and 661 cm^{-1} correspond to the aromatic amine C-N and aldehyde moiety of C-I stretching vibrations respectively. The aromatic C=C stretching vibrations are appeared at 1580, 1501 and 1473 cm^{-1}. The aromatic C-C stretching vibrations are exhibited at 1491 and 1453 cm^{-1}. A strong band at 1243–1261 cm^{-1}can be assigned to phenolic C-O stretching.

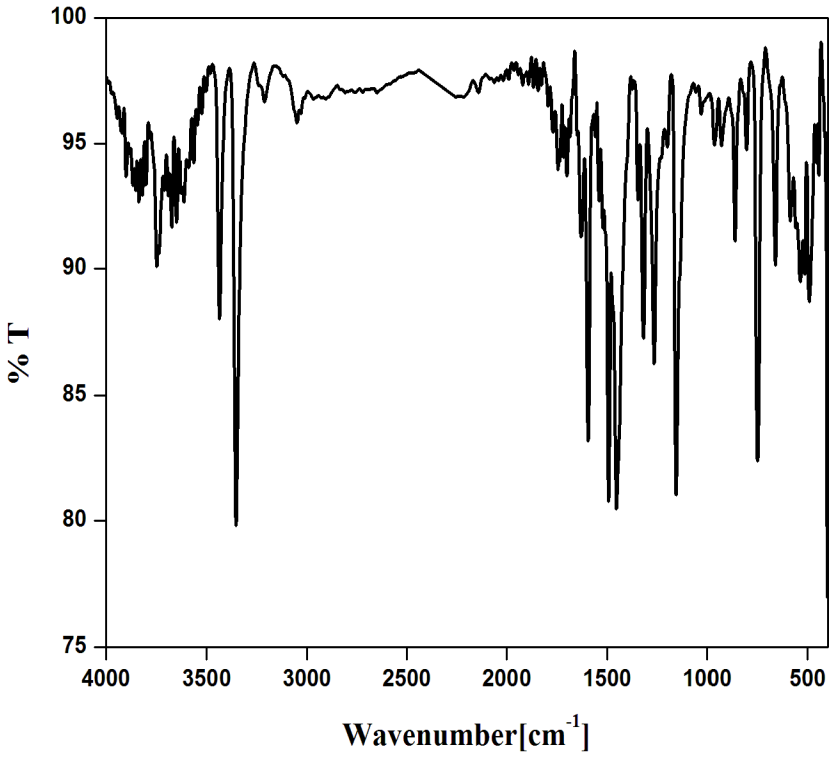

Fig. 5 shows the IR spectrum of PMDP

©IJRASET (UGC Approved Journal): All Rights are Reserved

Table II FT-IR SPECTRUM ASSIGNMENT OF PMDP

Frequencies (cm^{-1})	Assignment
3747, 3437	O-H stretching vibration
3354	C-H stretching vibration in aromatic ring
1593	C=N symmetric stretching vibration
1580, 1501, 1473	Aromatic C=C stretching vibration
1491, 1453	C-C symmetric stretching vibration
1154	C-N symmetric stretching vibration
862	C-H bending vibration
751	C-H bending vibration
661	C-I stretching vibration

5) Electronic spectral features : UV–Visible absorption spectrum of PMDP in methanol solvent was recorded and shown in Fig .6 The spectrum exhibits the blue region and the characteristic absorption band at 325 and 400 nm attributed to the π-π* and n-π* bands of the title compound.

The emission spectrum was recorded in methanol solvent and is shown in Fig. 6. The spectrum shows broad peak at 529 nm when excited at 400 nm. This covers the intact red regions of the visible spectrum.

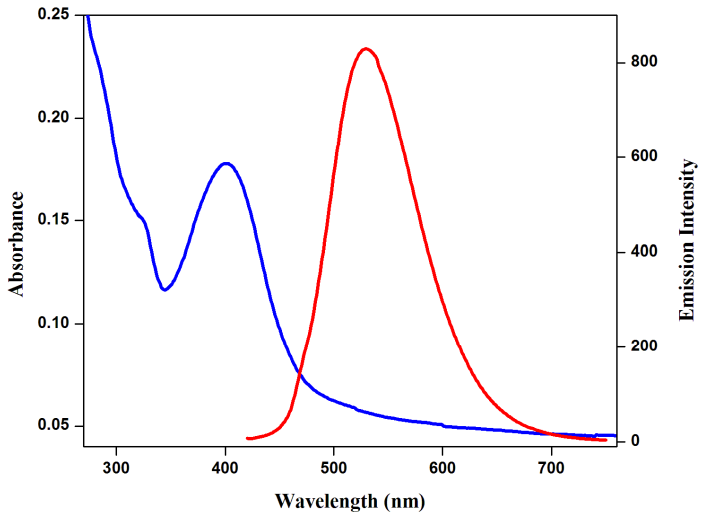

Fig. 6. UV–Visible absorption spectrum of PMDP

6) Thermal studies : Thermo gravimetric and differential thermal studies were used to examine the thermal stability of PMDP crystals and the recorded thermogram is shown in Fig. 7. The TG curve illustrated the absence of any detectable weight loss upto 281° C and the crystal material decomposed immediately after melting. The decomposition takes place gradually in the high temperature in a single stage into volatile gaseous products like NO_2, NH_3 and HI. The residue which remains after the decomposition may be a stable carbon compound. The DTA curve indicated the same changes shown by TG curve. The sharp

©IJRASET (UGC Approved Journal): All Rights are Reserved

endothermic dip at 281º C indicates the melting point of the material. The sharpness of this endothermic peak shows good degree of crystallinity and purity of the material. This is further confirmed by a melting point apparatus.

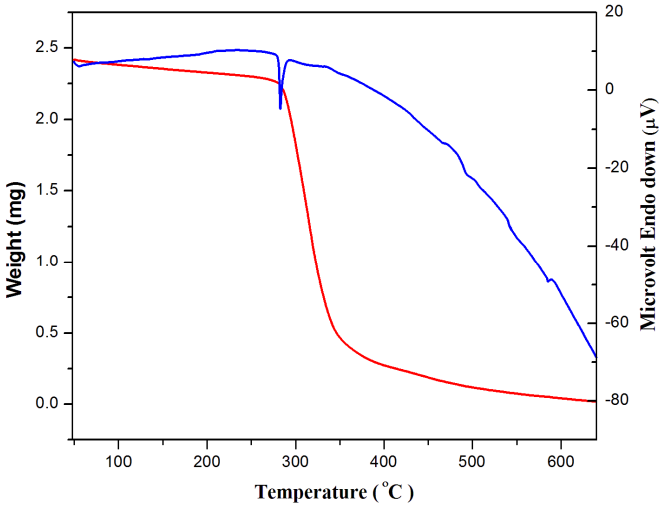

Fig. 7. Thermogram of PMDP

B. Computational investigation: As mentioned in experimental part, all calculations were carried out in B3LYP method in 6-311++G(d,p) basis set. The optimized structure of PMDP is shown in Fig. 8. The figure shows the molecule in the ball and stick model. The geometry optimization yields non planar structure. The optimized structural parameters of PMDP calculated by B3LYP/6- 311++G(d,p) are presented in Table III.

TABLE III THE OPTIMIZED STRUCTURAL PARAMETERS OF PMDP

Compound	KMD180
HOMO	-3.7888
LUMO	-2.3414
Energy gap	1.4474
IP	3.7888
EA	2.3414
Electronegativity(χ)	3.0651
μ	-3.0651
Hardness(η)	0.7237
Softness(σ)	1.3818
(ω)	6.4908
Etotal	-28427.24
Dipole moment	5.3216

©IJRASET (UGC Approved Journal): All Rights are Reserved

1) Electronic properties: Highest Occupied Molecular Orbital (HOMO) and Lowest Unoccupied Molecular Orbital (LUMO) known as Frontier Molecular Orbitals (FMO's) and their energy gap (Eg) are very useful parameters in quantum chemistry. HOMO can be thought as the outermost orbital which contains electrons representing the ability to donate an electron, while LUMO can be thought the innermost orbital containing free places representing the ability to accept an electron [26]. Lower HOMO-LUMO energy gap value indicates both the intra molecular charge transfer (ICT) within the molecule and lower chemical reactivity implying higher kinetic stability [27-29]. Both HOMO and LUMO are the main orbitals that take part in chemical stability. The HOMO-LUMO are computed at B3LYP/6-311G(d) level of theory [29].

In order to evaluate the energetic behavior of the synthesized PMDP, the HOMO and LUMO energy calculated by B3LYP method in 6-311++G(d,p) basis set is presented in Table. 3. Fig. 9. and Fig. 9A. shows the frontier molecular orbitals of the PMDP. The HOMO is localized on whole the four iodine atoms, oxygen atom of the two hydroxyl group and aldehyde benzene ring with strong contribution. Azomethine nitrogen (>C=N–) and carbon atom of the diamino benzene with weak contribution. The LUMO is localized mainly on the Azomethine nitrogen (>C=N–), the diamino benzene ring with great contribution, oxygen atom of the two hydroxyl group and aldehyde benzene moiety with weak contribution According to calculation, the energy band gap of PMDP reveals about 1.4474 eV by B3LYP method at the mentioned basis set.

HOMO energy = -3.7888 eV,
LUMO energy = -2.3414 eV.
HOMO-LUMO energy gap = 1.4474 eV

This small energy gap confirms the compounds with high chemical reactivity as well as high polarizability.

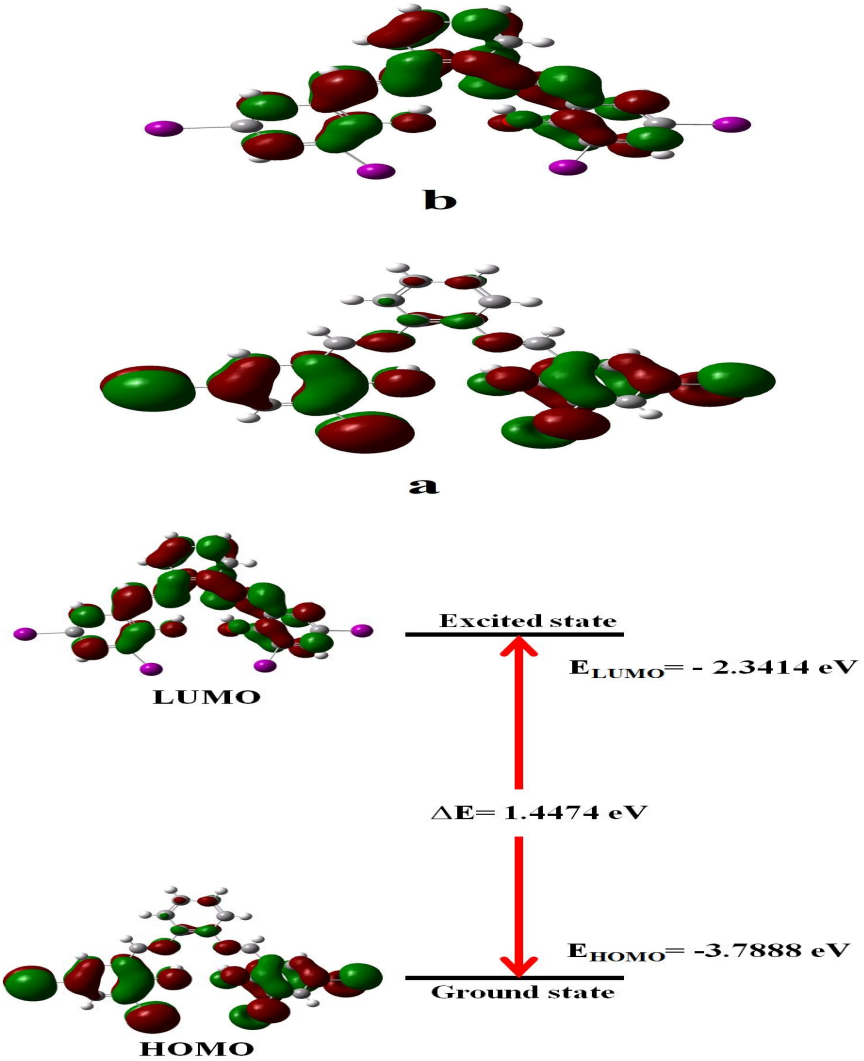

Fig. 9. and Fig. 9A. shows the frontier molecular orbitals of the PMDP

©IJRASET (UGC Approved Journal): All Rights are Reserved

2) Mulliken atomic charge: In order to evaluate the energetic behavior of the PMDP, we carried Mulliken atomic charge calculation has an important role in the application of quantum chemical calculation to molecular system because of atomic charges effect dipole moment, molecular polarizability, electronic structure and more a lot of properties of molecular systems [30]. The calculated Mulliken charge values of PMDP are listed in Table. IV. The charge changes with methods presumably occur due to variation of the hybrid functional. Illustration of atomic charges plotted is shown in Fig. 10. In compound all hydrogen atoms have a net positive charge. The obtained atomic charge shows that the H6 atom has bigger positive atomic charge (0.3327 e) than the other hydrogen atoms. This is due to the presence of electronegative oxygen atom (O5), the oxygen (O5) atom has bigger negative atomic charge (-0.32149 e) than the other oxygen atoms. The charge of the nitrogen atoms N9 and N10 in imine groups are -0.2628 e and -0.2507 e respectively. The oxygen atoms in hydroxyl group and nitrogen atoms in azomethine groups exhibit a negative charge, which are donor atoms [31].

TABLE. 4. MULLIKEN CHARGE VALUES OF PMDP

S.No	Atom	Charge
1	I	0.083878
2	I	0.063171
3	I	0.093966
4	I	0.071128
5	O	-0.321488
6	H	0.332735
7	O	-0.317752
8	H	0.331498
9	N	0.262801
10	N	-0.250766
11	C	0.079308
12	C	0.087346
13	C	-0.123303
14	H	0.114077
15	C	-0.102533
16	H	0.115679
17	C	-0.105379
18	H	0.114587
19	C	-0.116812
20	H	0.111947
21	C	-0.008260
22	H	0.110049

3) Molecular Electrostatic Potential: The MEP 3-D plots of PMDP are portrayed in Fig. 11. MEP was calculated at the B3LYP/6-311G(d,p) optimized geometry of the PMDP. The negative electrostatic potential in the molecule corresponds to an attraction of the proton by the concentrated electron density (red shades as EPS surface), the positive electrostatic potential correlate with the repulsion of the proton by atomic nuclei in regions where low electron density occurs and the nuclear charge is incompletely shielded (blue shades) [32, 33]. The different values of the electrostatic potential are represented by different colors. Potential increases in the order red < orange < yellow < green < blue. The significance of MEP lies in the fact that it simultaneously displays molecular size, shape as well as positive, negative and neutral electrostatic potential regions in terms of color grading and is very useful in research of molecular structure with its physiochemical property relationship. The red color is correlated with electron rich

©IJRASET (UGC Approved Journal): All Rights are Reserved

area whereas the blue color represents the electropositive sites [22, 33, 34]. ESP plots clearly indicate the maximum negative (red) region is localized on the hydroxyl oxygen probably due attached with benzene and iodine, maximum positive (blue) region is localized on outside of the benzene probably due to the hydrogen atoms. The color code of these maps is in the range between -5.202e^{-3} (deepest red) to 5.202e^{-3} (deepest blue) in PMDP, where blue indicates the strongest attraction and red indicates the strongest repulsion.

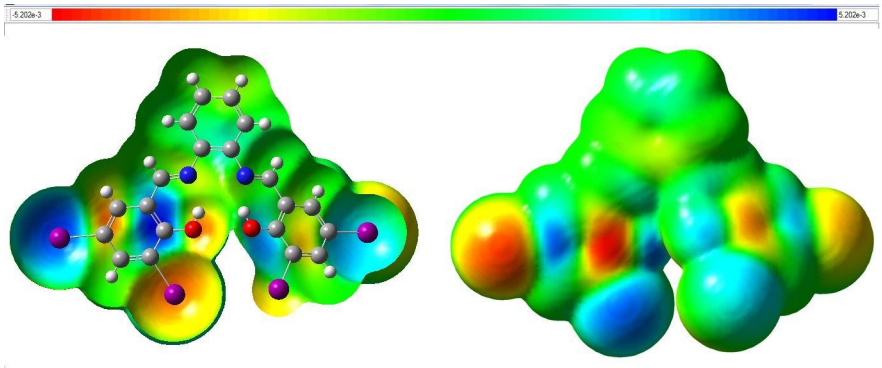

Fig. 11. MEP of PMDP

III. CONCLUSION

Single crystal of PMDP was successfully grown by slow evaporation solution growth technique at ambient temperature. The crystal structure was monoclinic crystal system with space group P21/n established by single crystal XRD analysis. The presence of various functional groups in the salt crystal has been confirmed by FT-IR spectroscopic study. The synthesized PMDP has good stabilities and their thermal decomposition temperature is 281 °C and it can be use in high temperature applications. This PMDP is found to have excellent optical properties. The Mulliken atomic charges as well as molecular electrostatic potential of the title compounds were reported. All the theoretical calculations were carried out by the more popular DFT methods, B3LYP, at 6-311++G(d,p) level of theory. The HOMO-LUMO energy gap as an important value for stability index revealed high chemical reactivity of synthesized PMDP in chemical reactions and the theoretical and experimental energy gap values indicate that the PMDP is suitable for the fabrication processes for optoelectronic devices.

This research did not receive any specific grant from funding agencies in the public, commercial, or not-for-profit sectors.

A. Supplementary data

Crystallographic data for the structural analysis have been deposited with the Cambridge Crystallographic Data Centre, CCDC 1011768. Copy of this information may be obtained free of charge from the Director, CCDC, 12 Union Road, Cambridge, CB21 EZ, UK (fax: +44 1223 336033: e-mail: deposit@ccdc.cam.ac.uk or www.ccdc.cam.ac.uk/deposit).

REFERENCES

[1] J. L. Segura, M. J. Mancheno, F. Zamora, Covalent organic frameworks based on Schiff-base chemistry: synthesis, properties and potential applications, Chem. Soc. Rev. 45 (2016) 5635-5671.
[2] O. R. Berny, S. O. Flores, I. Cordova, M. A. Valenzuela, Synthesis of imines from nitrobenzene and TiO_2 particles suspended in alcohols via semiconductor photocatalysis type B, Tetrahedron Lett. 51 (2010) 2730–2733.
[3] C. D. Meyer, C. S Joiner, J. F. Stoddart, Template-directed synthesis employing reversible imine bond formation, Chem. Soc. Rev. 36 (2007) 1705–1723.
[4] C. M. da Silva, D. L. da Silva, L. V. Modolo, R. B. Alves, M. A. de Resende, C. V. B. Martins, A. de Fatima, Schiff bases: A short review of their antimicrobial activities, J. Adv. Res. 2 (2011) 1–8.
[5] M. T. Cocco, C. Congiu, V. Lilliu, V. Onnis, Synthesis and in vitro antitumoral activity of new hydrazinopyrimidine-5-carbonitrile derivatives, Bioorg. Med. Chem. 14 (2006) 366–372.
[6] J. R. Hwu, C. C. Lin, S. H. Chuang, K. Y. King, T. R. Su, S. C. Tsay, Aminyl and iminyl radicals from arylhydrazones in the photo-induced DNA cleavage, Bioorg. Med. Chem. 12 (2004) 2509– 2515.
[7] B. S. Creaven, B. Duff, D. A. Egan, K. Kavanagh, G. Rosair, V. R. Thangella, M. Walsh, Anticancer and antifungal activity of copper(II) complexes of quinolin-2(1H)-one-derived Schiff bases, Inorg. Chim. Acta. 363 (2010) 4048-4058.
[8] K. Singh, M. S. Barwa, P. Tyagi, Synthesis, characterization and biological studies of Co(II), Ni(II), Cu(II) and Zn(II) complexes with bidentate Schiff bases derived by heterocyclic ketone, Eur. J. Med. Chem. 41 (2006) 147–153.
[9] J. Zhao, Y. Xie, D. Hu, D. Guan, J. Chen, J. Yu, S. He, Y. Lu, H. Liu, S. Bao, L. Wang, Phenylenediamine–benzaldehyde Schiff base Ag(I) complexes grown on graphene with the intercalated structures for electromagnetic composites, Synth. Met. 204 (2015) 95–102.

©IJRASET (UGC Approved Journal): All Rights are Reserved

[10] O.E. Sherif, N. S. A. Kader, Spectroscopic and biological activity studies of bivalent transition metal complexes of Schiff bases derived from condensation of 1,4-phenylenediamine and benzopyrone derivatives, Spectrochim. Acta. Mol. Biomol. Spectrosc. 117 (2014) 519–526.
[11] J. Balaji, S. Prabu, P. Srinivasan, (E)-N'-(4-chlorobenzylidene)-4-methylbenzenesulfonohydrazide (4CBTH) – Synthesis and characterization of organic NLO crystal, J. Crys. Growth 452 (2016) 189-197.
[12] A. Koll, Specific Features of Intramolecular Proton Transfer Reaction in Schiff Bases, Int. J. Mol. Sci. 4 (2003) 434-444
[13] S. Manivannan, S. Dhanuskodi, Synthesis, crystal growth, structural and optical properties of an organic NLO material, J. Crys. Growth 262 (2004) 473–478.
[14] B. S. Furniss, A. J. Hannaford, P. W. G. Smith, A. R. Tatchell, Vogel's Text Book of Practical Organic Chemistry, fifth ed., Longman, London, 1989.
[15] G. M. Sheldrick, A short history of SHELX, Acta Crystallogr. Sect. A. 64 (2008) 112–122.
[16] A.L. Spek, Single-crystal structure validation with the program Platon, J. Appl. Crystallogr. 36 (2003) 7–13.
[17] A. D. Becke, Densityfunctional thermochemistry III. The role of exact exchange, J. Chem. Phys. 98 (1993) 5648-5652.
[18] Z. D. Petrovic, J. Dorovic, D. Simijonovic, V. P. Petrovic, Z. Markovic, Experimental and theoretical study of antioxidative properties of some salicylaldehyde and vanillic Schiff bases, RSC Adv. 5 (2015) 24094–24100.
[19] Z. Parsaee, K. Mohammadi, M. Ghahramaninezhad, B. Hosseinzadeh, A novel nano-sized binuclear nickel(II) Schiff base complex as a precursor for NiO nanoparticles: synthesis, characterization, DFT study and antibacterial activity, New J. Chem. 40 (2016) 10569-10583.
[20] M. Shkir, S. Muhammad, S. AlFaify, A. Irfan, P.S. Patil, M. Arora, H. Algarni, J.P. Zhang, Investigation on the key features of D-π-A type novel chalcone derivative for optoelectronic applications, RSC Adv. 5 (2015) 87320–87332.
[21] A. J. Cohen, P. M. Sanchez, W. Yang ,Challenges for Density Functional Theory, Chem. Rev. 112 (2012) 289–320.
[22] S. Kamalesu, K. Swarnalatha, R. Subramanian, K. Muralidharan, S. Gomathi, Polypyridyl-hydrazone based Ruthenium(II) complexes: Spectral and computational analysis, Inorg. Chim. Acta 461 (2017) 35–44.
[23] C. J. Cramer, D. G. Truhlar, Density functional theory for transition metals and transition metal chemistry, Phys. Chem. Chem. Phys. 11 (2009) 10757–10816.
[24] X. L. Gao, L. P. Lu, M. L. Zhu, The crucial role of C—HO and COp interactions in the building of three-dimensional structures of dicarboxylic acid–biimidazole compounds, Acta. Cryst. C 65 (2009) 123–127.
[25] R. M. Kumar, M. Elango, R. Parthasarathi, D. Vijay, V. Subramanian, The role of C–H...π interaction in the stabilization of benzene and adamantane clusters, J. Chem. Sci. 124 (2012) 193–202.
[26] M. Kurt, E. B. Sas, M. Can, S. Okur, S. Icli, S. Demic, M. Karabacak, T. Jayavarthanan, N. Sundaraganesan, Synthesis and spectroscopic characterization on 4-(2,5-di-2-thienyl- 1H-pyrrol-1-yl) benzoic acid: A DFT approach, Spectrochim. Acta - Part A Mol. Biomol. Spectrosc. 152 (2016) 8–17.
[27] A. M. Zalas, J. Luc, B. Sahraoui, I.V. Kityk, Kinetics of third-order nonlinear optical susceptibilities in alkynyl ruthenium complexes, Opt. Mater. 28 (2006) 1147-1151.
[28] C. Ravikumar, I. Hubert Joe, V.S. Jayakumar, Charge transfer interactions and nonlinear optical properties of push–pull chromophore benzaldehyde phenylhydrazone: A vibrational approach, Chem. Phys. Lett. 460 (2008) 552-558.
[29] M. Govindarajan, M. Karabacak, Spectroscopic properties, NLO, HOMO–LUMO and NBO analysis of 2,5-Lutidine, Spectrochim Acta A. 96 (2012) 421-435.
[30] H. Ebrahimi, J. S. Hadi, H. S. Al-Ansari, Spectroscopic properties, NLO, HOMO–LUMO and NBO analysis of 2,5-Lutidine , J. Mol. Struct. 1039 (2013) 37-45.
[31] L. Arrue, M. Rey, C. R. Hernandez, S. Correa, E. Molins, L. Norambuena, X. Zarate, E. Schott, Synthesis, characterization, spectroscopic properties and DFT study of a new pyridazinone family, J. Mol. Struct. 1148 (2017) 162-169.
[32] T. Yesilkaynak, G. Binzet, F.M. Emen, U. Florke, N. Kulcu, H. Arslan, Theoretical and experimental studies on N-(6-methylpyridin-2-yl-carbamothioyl)biphenyl-4-carboxamide, Eur. J. Chem. 1 (2010) 1-5.
[33] S. Mishra, D. Chaturvedi, N. Kumar, P. Tandon, H.W. Siesler, An ab initio and DFT study of structure and vibrational spectra of Y form of Oleic acid: Comparison to experimental data, Chem. Phys. Lipids 163 (2010) 207-217.
[34] S. Karmakar, S. Mardanya, D. Maity, S. Baitalik, Polypyridyl-imidazole based Os(II) complex as optical chemosensor for anions and cations and multi-readout molecular logic gates and memory device: Experimental and DFT/TDDFT study, Sensors Actuators B. Chem. 226 (2016) 388-402.

©IJRASET (UGC Approved Journal): All Rights are Reserved

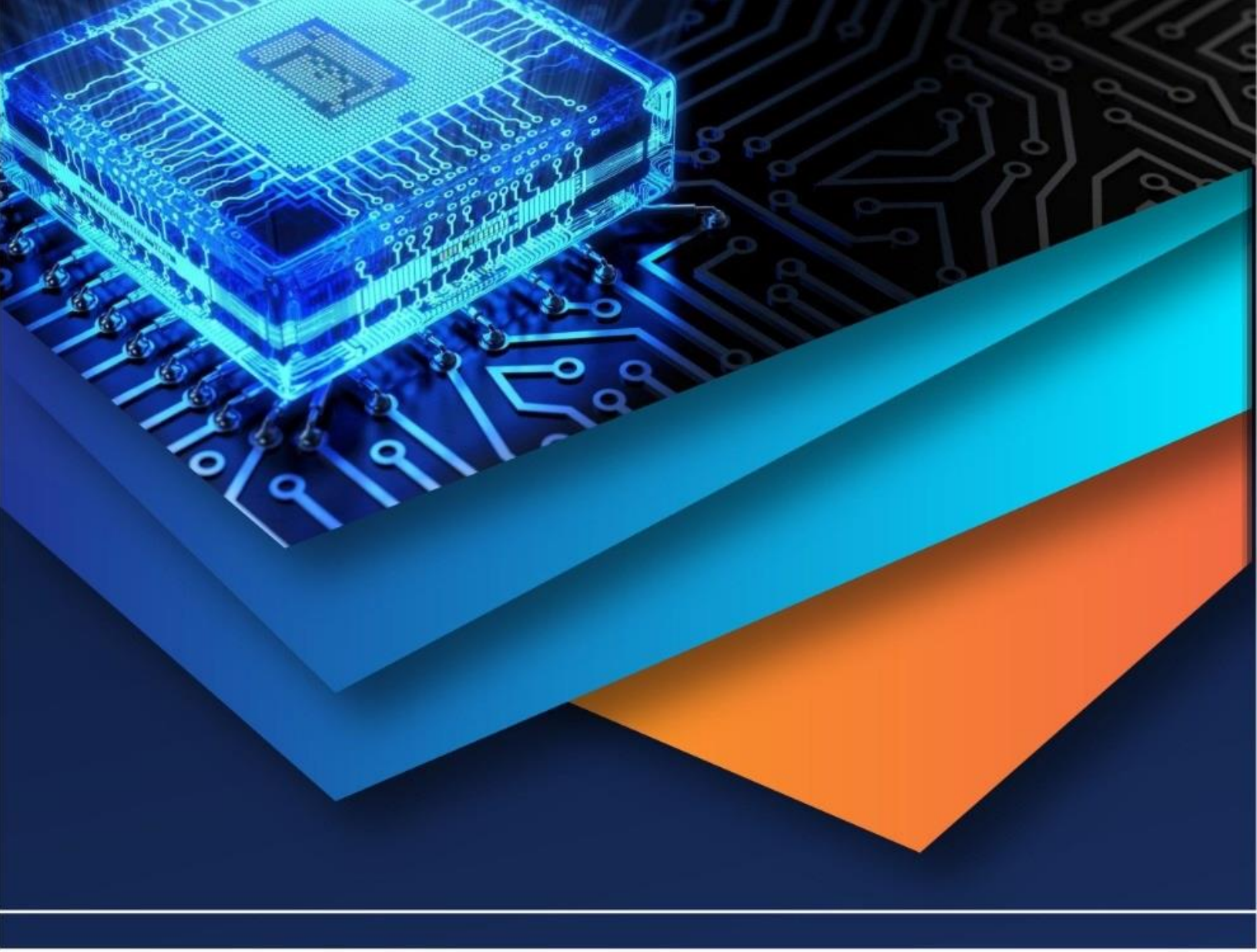

10.22214/IJRASET

45.98

IMPACT FACTOR: 7.129

IMPACT FACTOR: 7.429

INTERNATIONAL JOURNAL FOR RESEARCH

IN APPLIED SCIENCE & ENGINEERING TECHNOLOGY

Call : 08813907089 (24*7 Support on Whatsapp)